INSTITUTE OF PHYSICS PUBLISHING JOURNAL OF PHYSICS B: ATOMIC, MOLECULAR AND OPTICAL PHYSICS

J. Phys. B: At. Mol. Opt. Phys. **36** (2003) 2019–2032 PII: S0953-4075(03)58862-9

Electron impact ionization of Kr XI–Kr XIX ions

I Beigman[1], **P Defrance**[2] **and L Vainshtein**[1]

[1] Lebedev Physical Institute, Leninsky Avenue, 53, 119991, Moscow, Russia
[2] Department of Physics (FYAM) 2, Chemin du Cyclotron, B-1348 Louvain-la-Neuve, Belgium

Received 26 November 2002, in final form 1 April 2003
Published 6 May 2003
Online at stacks.iop.org/JPhysB/36/2019

Abstract

Cross sections for the single ionization of Kr XI–XIX ions by electron impact are calculated in the Coulomb–Born approximation by the code 'ATOM' and compared with experimental data and other theoretical results for Kr XI, Kr XII and Kr XIX. Single electron impact ionization is the sum of the contributions from direct ionization and from excitation of the autoionizing levels. The first part includes only ionization from the 3s, 3p and 3d shells since ionization from the 1s, 2s, 2p shells results in double ionization. The autoionizing levels ($1s^2 2s 2p^6 3s^2 3p^6 3d^m nl$ and $1s^2 2s^2 2p^5 3s^2 3p^6 3d^m nl$) decay via autoionization and finally contribute to single ionization. The results are found to be in satisfactory agreement with the experimental results obtained in a crossed electron–ion beam experiment in the energy range from threshold to about 6 keV. The case of ions formed in metastable states is studied as they were observed experimentally.

1. Introduction

In the design of future thermonuclear reactors, krypton has been recognized as a good candidate for the spectroscopic diagnostics of, for instance, the temperature in the plasma edge, as well as in the central plasma. For this reason, a good knowledge of related spectroscopic and collisional atomic data is needed in order to interpret the observations of various plasma parameters (Janev 1993). Among the processes playing a role in this field, electron-impact ionization of atoms and ions is a fundamental one, because it governs the ion charge state distribution evolution in the plasma. As a consequence, the corresponding ionization cross sections are required for plasma modelling.

For single ionization, experimental cross sections for Kr XI–XIX have been published. In particular, the largest charge states were studied in the laboratory of Louvain-la-Neuve for Kr XI, Kr XII (Oualim *et al* 1995) and Kr XIII–XIX (Khouilid *et al* 2001a) in the energy range from subthreshold to about 6 keV. In the experiment, the animated crossed-beams method is applied in an apparatus (Duponchelle *et al* 1995) specially designed to study electron-impact ionization (single and multiple) of multiply charged ions (X^{q+}) up to $q = 20$. The krypton ions are extracted from an electron cyclotron resonance ion source (Barué *et al* 1998) and are accelerated by a voltage of some kilovolts, mass-analysed, focused and deflected to the

0953-4075/03/102019+14$30.00

Table 1. Ionization energies (eV).

Hole	1s(1/2)	2s(1/2)	2p(1/2)	2p(3/2)	3s(1/2)	3p(1/2)	3p(3/2)	3d(3/2)	3d(5/2)
Kr IX	14 474.5	2074.55	1876.67	1823.75	434.665	363.913	355.79	232.61	231.33
Kr XIX	15 033.4	2631.44	2435.43	2381.91	869.374	795.344	784.406		

Table 2. (a) Ionization energies (eV) for Kr IX–Kr XIX that were averaged over the upper configuration terms. (b) Minimal ionization energies (eV) for Kr IX–Kr XIX (Z is the spectroscopic symbol).

	Z	1s	2s	2p	3s	3p
(a)	9	14 475	2074.6	1841.4	434.7	358.5
	10[a]	14 530	2130.6	1899.1	482.8	407.1
	11[a]	14 584	2184.8	1954.1	528.1	452.3
	12[a]	14 636	2237.7	2007.2	571.2	494.9
	13[a]	14 688	2290.0	2059.3	612.8	535.6
	14	14 741	2342.5	2111.2	653.5	575.4
	15[a]	14 794	2395.7	2163.8	694.1	615.0
	16[a]	14 849	2450.4	2218.0	735.2	655.1
	17	14 907	2507.3	2274.8	777.3	696.6
	18	14 968	2567.0	2334.9[c]	821.3	740.2
	19	15 033	2631.4	2399.8	869.4	788.0
	19[b]	15 049	2640.0	[2410]	876.9	799.8
(b)	9	14 475	2074.6	1823.8	434.7	355.8
	10[a]	14 519	2115.5	1864.6	465.7	386.1
	11[a]	14 566	2160.5	1909.5	500.6	419.9
	12[a]	14 616	2209.0	1958.2	538.9	457.0
	13[a]	14 668	2261.1	2010.4	580.3	496.9
	14	14 722	2316.3	2065.6	624.3	539.3
	15[a]	14 779	2374.4	2123.5	670.4	583.9
	16[a]	14 839	2435.3	2183.8	718.3	630.4
	17	14 901	2498.5	2246.1	767.7	678.3
	18	14 966	2563.9	2310.0	817.9	727.4
	19	15 033	2631.4	2381.9	869.4	784.4
	19[b]	15 049	2624.5	[2390]	856.4	781.7

[a] Values were interpolated over Z.
[b] Data for metastable Kr XIX ($3p^5 3d$); $I(2p)$ is estimated.
[c] Double ionization experiment (Khouilid *et al* 2001b) gives a value of 2335(5) eV.

collision region where the crossing with the electron beam takes place. A magnetic mass analyser separates the product ions from the primary ions.

The structure of the ions under consideration is of the form $[Ar]3d^m$ ($m = 0$–8). For Kr XIII, Kr XV, Kr XVII and Kr XIX important signals were observed below the ground-state ionization threshold indicating the presence of metastable states in the primary ion beam. The metastable state may be identified from the comparison of the experimental and calculated values of the ionization threshold. Energy thresholds corresponding to ionization and excitation of outer shell or inner-shell electrons were estimated from the Hartree–Fock structure calculation (Blanke *et al* 1992). The observed metastable state belongs to the ground configuration for Kr XIII, Kr XV and Kr XVII. For Kr XIX, which belongs to the argon isoelectronic sequence, the lowest excited configuration $3p^5 3d$ is observed.

In the experiments, the respective role of direct and indirect processes was analysed in detail. Theoretical cross sections have been obtained for charge states 10–11 (Teng *et al*

Table 3. Comparison of the 3d ionization energies (eV) (Z is the spectroscopic symbol).

Z	Bl.	Exp.	I_{min}	I_{av}
9		230.97[b]	231.3	231.8
10[a]		268.18[b]	270.5	280.3
11[a]	314.0	314(1)	311.9	326.5
12[a]	360.0	360(1)	355.1	371.2
13[a]	400.(2)	401(1)	400.0	414.8
14	449.6	446(2)	446.2	458.0
15[a]	491.8[e]	478(3)[c]	493.6	501.5
16[a]	542.8	542(3)	541.8	545.9
17	593.0	585(5)[c]	590.6	591.7
18	641.3	637(5)	639.7	639.7
19[d]	700.2	703(10)	696.7	700.4

[a] Values were interpolated over Z.
[b] NIST data (Kelleher *et al* 2002).
[c] Metastable state.
[d] 3d metastable state.
[e] Sugar and Musgrove 1991.

Table 4. The ionization and excitation energies for the autoionization levels (eV) used.

Z	I 3d	I 3p	I 3s	E(2p–3d)	E(2s–3d)	E(3s–nl)	E(3p–nl)
11	313.9	452.1	527.9	1615	1870	328.6(4s)	343.4(4f)
12	359.9	494.7	571.0	1622	1877	400.9(4d)	380.8(5p)
13	400.9	535.5	612.6	1633	1888	418.3(4d)	405.9(4f)
14	445.8	575.2	653.3	1635	1896	496.1(5s)	445.7(5d)
15	477.8	614.8	693.9	1645	1917	519.3(5s)	502.3(6s)
16	545.7	654.9	734.9	1632	1904	552.8(5p)	553.7(6f)
17	584.8	696.3	777.1	1650	1922	594.0(5d)	598.8(7s)
18	639.3	739.9	821.0	1655	1927	712.9(7s)	662.0(8p)
19	703.0	799.5	876.5	1671	1843	757.7(7s)	730.8(9s)

2000) and 18 (Younger 1982, Khouilid *et al* 2001a) in the configuration-average distorted wave (CADW) approximation. Very recently, ionization cross sections for all the Kr ions were calculated by this method in Loch *et al* (2002).

This paper consists of two parts. In the first part the results of our calculations of ionization energies exploring the code GRASP2 (Grant *et al* 1980) are reported and compared with the data deduced from Blanke *et al* (1992) and from the experiments. In the second part, the cross sections calculated by the code ATOM (Shevelko and Vainshtein 1993) in the Coulomb–Born approximation are presented. In the framework of this approach the Coulomb attraction of the incident electron by ion is taken into account. It can be shown that the Coulomb–Born approximation (as well the distorted wave approximation) is asymptotically exact in the limit of a large ion charge. In the cross section calculations the energies given in the first part are used.

2. Results and discussion: energy

2.1. Ionization energies

The ionization energies were calculated in the one-configuration approximation by the GRASP2 code (Grant *et al* 1980) as the differences of the total energies of the initial and final states. Energies for all the shells for ions Kr IX–XIX were obtained. The results for

Table 5. Total single ionization cross section ($10^{-4}\pi a_0^2$, E in keV).

Z																			
11		12		13		14		15		16		17		18		19			
$3s^2 3p^6 3d^8$		$3s^2 3p^6 3d^7$		$3s^2 3p^6 3d^6$		$3s^2 3p^6 3d^5$		$3s^2 3p^6 3d^4$		$3s^2 3p^6 3d^3$		$3s^2 3p^6 3d^2$		$3s^2 3p^6 3d$		$3s^2 3p^5 3d$	
E	σ	E	σ	E	σ	E	σ	E	σ	E	σ	E	σ	E	σ	E	σ		
0.32	9.60	0.37	10.03	0.41	20.38	0.46	11.14	0.49	3.46	0.55	0.73	0.60	3.11	0.65	0.26	0.71	0.37		
0.33	40.71	0.38	20.16	0.42	32.35	0.48	40.24	0.52	21.02	0.58	16.63	0.62	10.66	0.71	10.10	0.75	5.60		
0.35	110.92	0.40	59.80	0.45	71.43	0.50	58.31	0.55	66.37	0.62	44.25	0.66	34.72	0.75	13.09	0.79	6.95		
0.40	214.47	0.45	153.36	0.50	144.25	0.55	101.52	0.58	68.74	0.66	49.13	0.70	35.20	0.80	17.62	0.81	7.77		
0.45	292.33	0.51	203.51	0.52	146.35	0.58	110.89	0.62	78.62	0.70	54.63	0.75	40.71	0.83	20.20	0.87	11.69		
0.51	331.94	0.54	213.16	0.54	156.86	0.62	120.26	0.66	86.12	0.80	66.83	0.80	45.50	0.90	25.91	0.90	13.84		
0.54	340.14	0.60	234.38	0.60	172.26	0.65	126.51	0.80	104.30	0.90	74.77	0.90	53.64	1.00	31.82	1.00	19.64		
0.60	356.53	0.70	251.74	0.70	192.57	0.70	135.88	0.90	110.62	1.00	79.35	1.00	58.19	1.20	37.53	1.20	25.78		
0.80	371.56	0.80	258.49	0.80	200.27	0.80	146.29	1.00	113.38	1.50	80.26	1.20	62.26	1.40	39.82	1.40	28.54		
1.00	355.17	1.00	256.56	1.00	203.07	1.00	153.58	1.50	108.25	1.62	79.04	1.50	61.78	1.50	40.20	1.50	29.01		
1.50	303.26	1.50	224.73	1.50	182.77	1.62	137.44	1.63	106.27	1.64	82.40	1.64	61.06	1.65	40.20	1.58	29.47		
1.60	295.06	1.60	218.94	1.62	175.76	1.65	138.48	1.66	107.85	1.66	82.09	1.67	65.13	1.68	45.53	1.61	29.93		
1.63	292.33	1.63	217.98	1.64	177.16	1.80	133.80	1.88	102.32	1.88	79.04	1.88	62.74	1.80	44.96	1.80	35.30		
1.80	278.67	1.80	207.37	1.80	170.16	1.90	132.24	1.90	102.72	1.90	78.74	1.90	62.50	1.90	44.20	1.90	34.99		
2.00	265.01	2.00	199.65	2.00	163.86	2.00	129.63	2.00	102.72	2.00	79.04	2.00	63.22	2.00	45.72	2.00	35.76		
2.50	232.22	2.50	175.54	2.50	144.25	2.50	115.58	2.50	91.65	2.50	72.02	2.50	58.67	2.50	43.82	2.50	35.60		
3.00	207.64	3.00	157.21	3.00	129.55	3.00	104.12	3.00	82.57	3.00	64.70	3.00	52.92	3.00	39.82	3.00	32.54		
5.00	147.53	5.00	112.85	5.00	93.13	5.00	74.97	5.00	59.26	5.00	47.30	5.00	38.55	5.00	29.34	5.00	24.09		

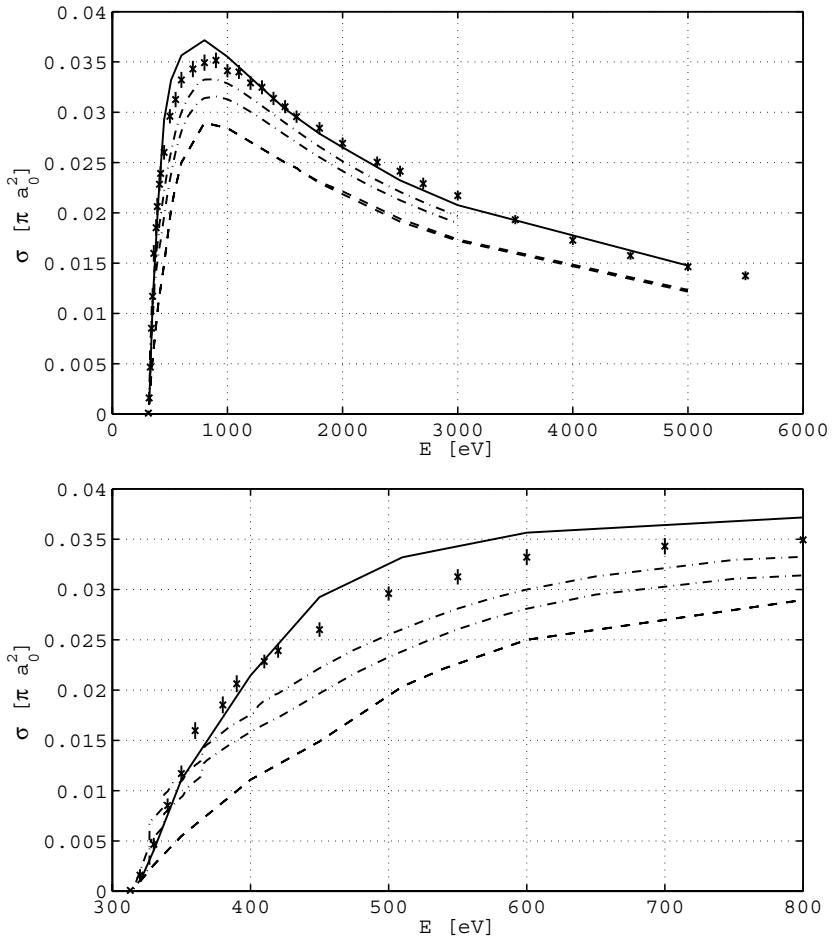

Figure 1. Ionization cross sections of Kr XI from the $3s^2 3p^6 3d^8$ state; '×', experimental data; solid curve, calculated total ionization cross section; the lower dashed curve represents direct ionization from the 3s, 3p, 3d shells only and, for the upper dashed curve, excitation from the 2s, 2p inner shells is added to the previous one; the calculations of Teng *et al* (2000) are represented by dash–dotted curves: total cross sections (upper curve) and direct ionization from the 3s, 3p, 3d shells only (lower curve).

the ground states of ions with closed shells (Kr IX and Kr XIX) are presented in the table 1. The ionization energies of the 3d electron in Kr IX and the 3p electron in Kr XIX are in good agreement with NIST (Kelleher *et al* 2002) data (230.97 and 785.94 eV, respectively).

The inner-shell ionization of ions with an open 3d shell gives many states of the next ion. The energies were averaged over upper configuration terms and used in our calculations by ATOM as target wavefunctions energetic parameters. These averaged energies are presented in table 2(a). The results for ions Kr X–XIII and Kr XV–XVI are obtained by interpolation by splines. The averaged ionization potential of the 2p shell of Kr XVIII is in good agreement with the experimental value 2335(5) eV from (Khouilid *et al* 2001b).

In the real ionization experiment, the minimal ionization potentials are the ones most frequently observed. They are given in table 2(b).

In table 3 the calculated and observed ionization energies for the 3d shell are compared. The column 'Blanke' gives the data from Blanke *et al* (1992) that were used for the classification

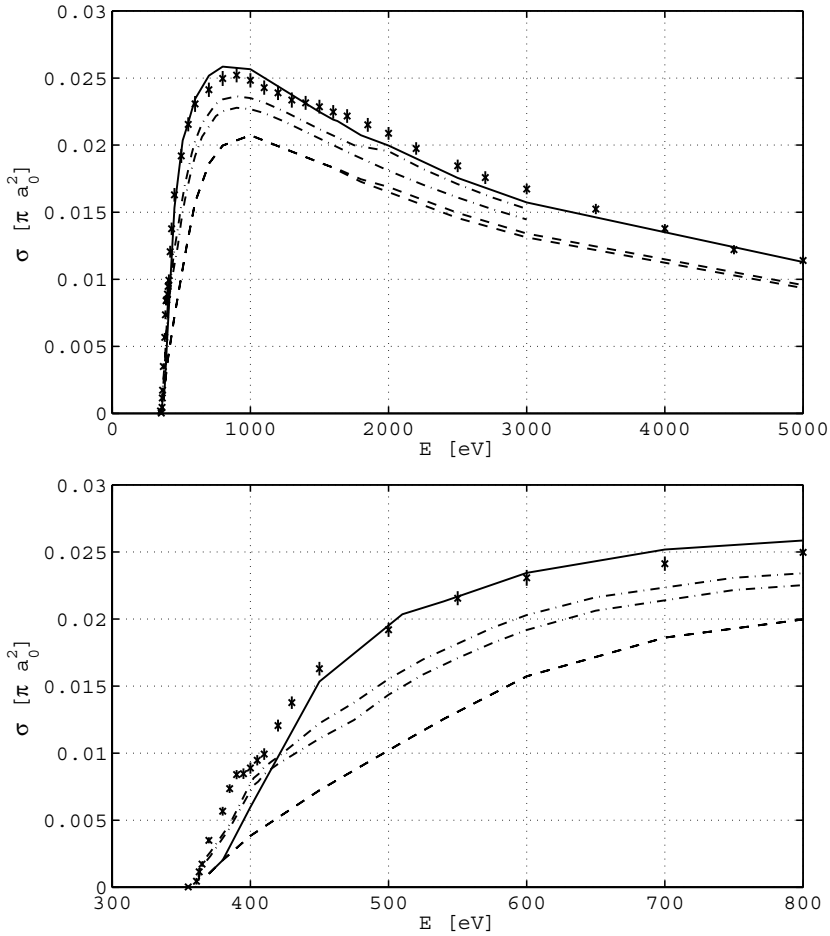

Figure 2. The same as figure 1 for Kr XII from the $3s^2 3p^6 3d^7$ state.

of the initial state. The observed energies (Khouilid *et al* 2001a) are given in the column 'Exp'. The last two columns include the minimal (I_{min}) and averaged (I_{av}) energy values calculated in the present work (tables 2(a), (b)). The disagreement between I_{min} and the experimental value is within the limits of the experimental error except Kr XII (difference 5 eV) and Kr XV, Kr XVII where the experimental data corresponds to the metastable states.

3. Results and discussion: ionization cross sections

A single ionization cross section is the sum of the contributions from direct ionization and from excitation of the autoionizing levels. Ionization from the 3s, 3p, 3d shells is direct ionization. Ionization from the 1s, 2s, 2p shells produces ions in autoionizing states which, after decay, gives doubly or triply ionized ions and therefore does not contribute to the single ionization process. The levels $1s^2 2s 2p^6 3s^2 3p^6 3d^m nl$ and $1s^2 2s^2 2p^5 3s^2 3p^6 3d^m nl$ (quantum numbers nl include 3d) after autoionization give the singly ionized ion. The radiative decay probability is much smaller than the autoionization one in this case (see also Teng *et al* 2000). Thus

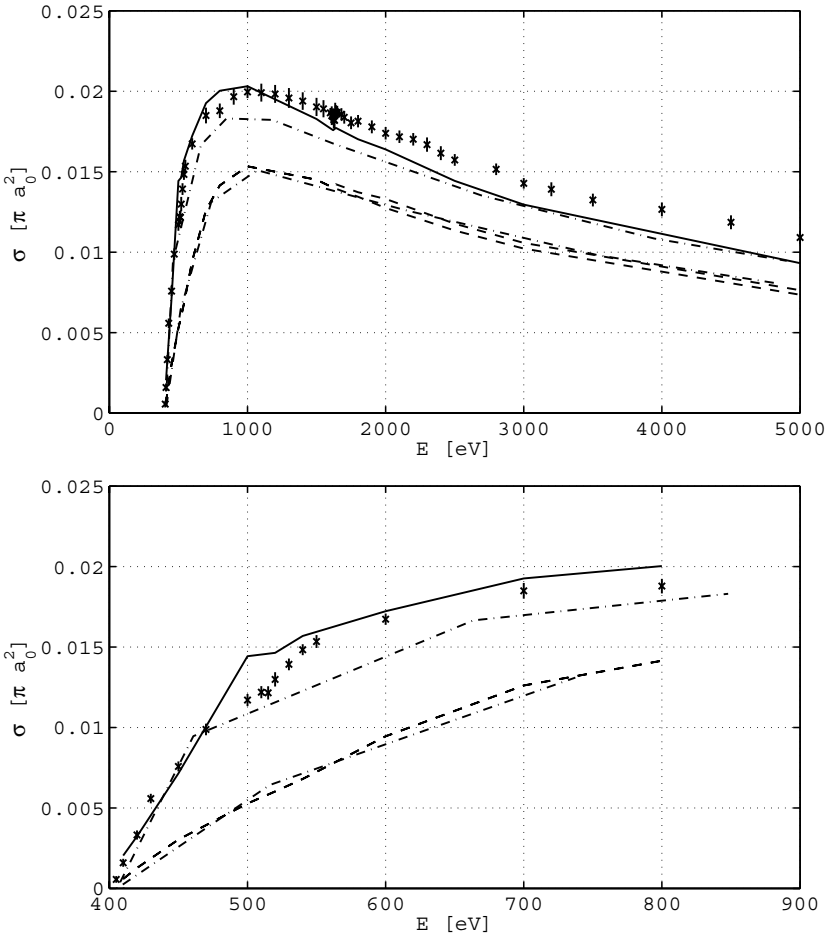

Figure 3. The same as figure 1 for Kr XIII from the $3s^2 3p^6 3d^6$ state; but the dash–dotted curves here represent the calculations of Loch *et al* (2002): total cross sections (upper curve) and direct ionization from the 3s, 3p, 3d shells only (lower curve).

the excitation of these levels gives the contribution to the single ionization process. We also assume that almost all the levels

$3s3p^6 3d^q nl$ and $3s^2 3p^5 3d^q nl$ (for Kr XI–XVIII),

$3s3p^5 3d^q nl$ and $3s^2 3p^4 3d^q nl$ (for Kr XIX)

with energies higher than the ionization limit also give singly ionized ions.

The ionization and excitation cross sections of Kr XI–XIX were calculated by the code 'ATOM' (Shevelko and Vainshtein 1993). The Coulomb–Born approximation with exchange was used (see details in Sobelman *et al* 1995). The target wavefunctions were in a one-electron approximation with energetic parameters equal to the ionization energies that were averaged over the upper configuration (see table 2(a)). The core potentials were scaled to obtain the eigenvalues of the target radial equation to be equal to the energetic parameters. The threshold energies used for the ionization and excitation are given in table 4. The two last columns of table 4 show the lowest autoionization level for the $3s3p^2 3d^m nl$ and $3s^2 3p3d^m nl$ series. The excitation cross sections for these levels were calculated directly. The contribution of the highest levels was estimated by the asymptotic $1/n^3$ law.

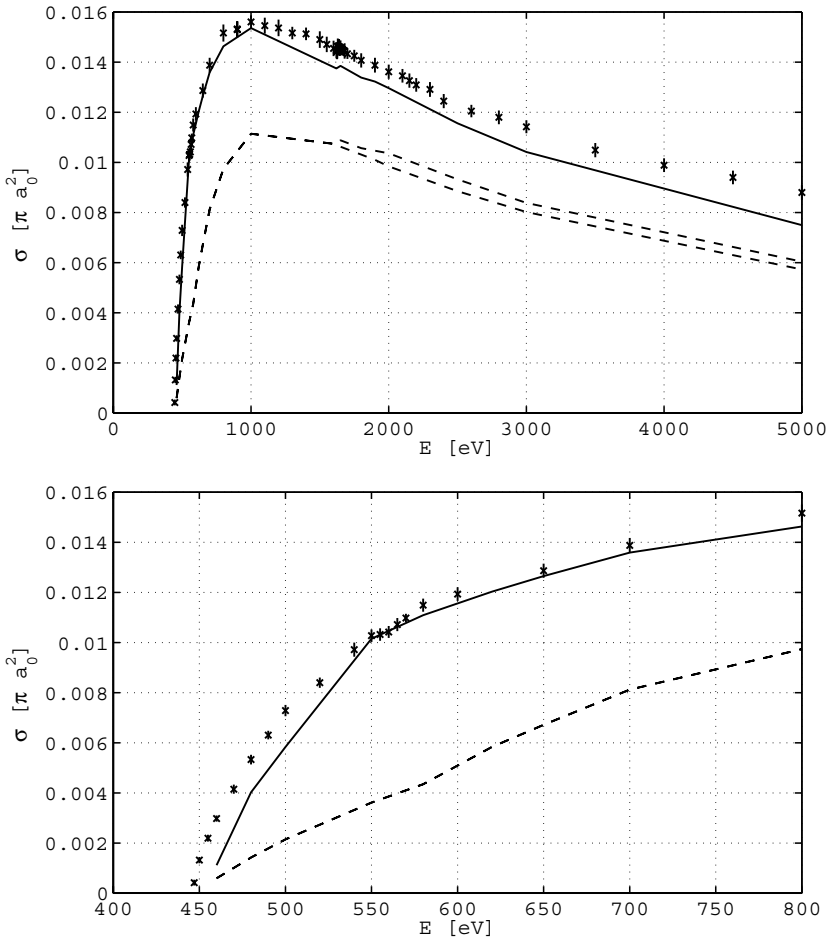

Figure 4. Ionization cross sections of Kr XIV from the $3s^2 3p^6 3d^5$ state; '$\times$', experimental data; solid curve, calculated total ionization cross section; the lower dashed curve represents direct ionization from the 3s, 3p, 3d shells only and, for the upper dashed curve, excitation from the 2s, 2p inner shells is added to the previous one.

The calculated total single ionization cross sections versus the incident electron energy E are presented in the figures 1–9 and in table 5.

3.1. Kr XI and Kr XII

The comparisons between the experimental data (Oualim *et al* 1995) and the previous calculations (Teng *et al* 2000) are presented in figures 1, 2. It should be noted that there is a very small contribution of autoionization from the 2s, 2p shells (very close dashed curves), and a significant contribution of excitation from the 3s, 3p shells. Near the threshold this excitation is the dominating process. We see good agreement with the experimental data at $E > 450$ eV. At smaller energies a complex structure takes place due to the excitation of the $n > 9$ levels. In our calculations their contribution was estimated on average. There is some difference (about 10%) between the present calculations and the results (Teng *et al* 2000).

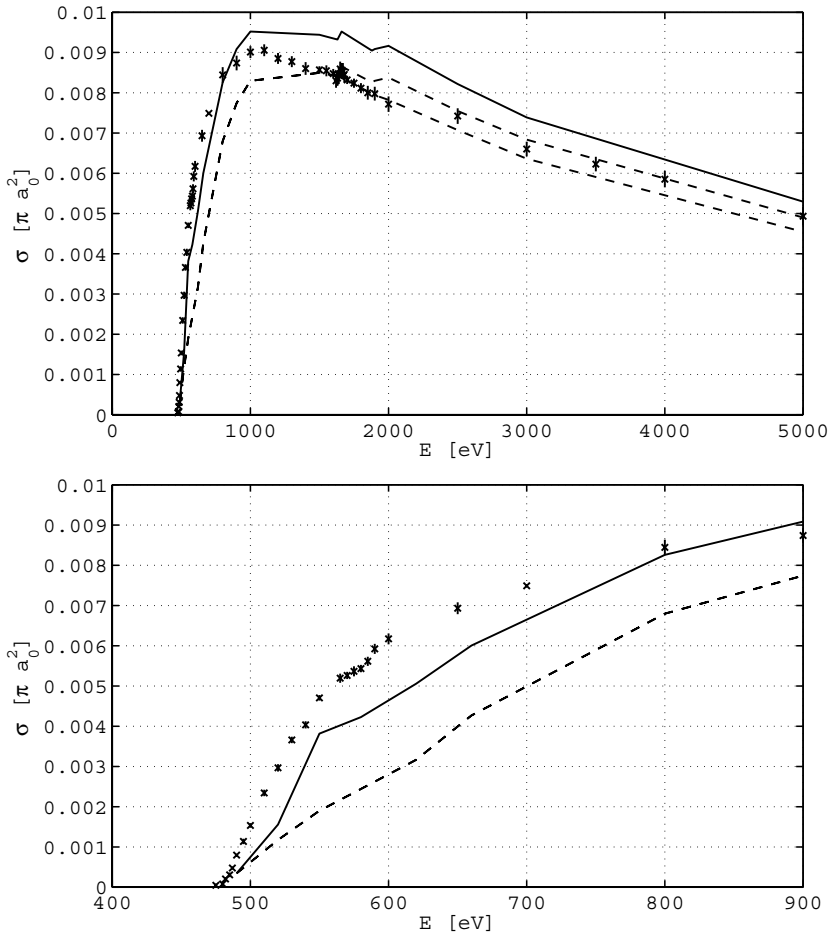

Figure 5. The same as figure 4 for Kr XV from the $3s^2 3p^6 3d^4$ state.

3.2. Kr XIII and Kr XIV

The comparison with the experimental data (Khouilid *et al* 2001a) is presented in figures 3, 4. Again the contribution of the autoionization from 2s, 2p shells is small, but slowly increases as compared to Kr XII. The contribution of the excitations from 3s, 3p shells is significant and dominates in the near threshold region (since its cross section is sharply increased at the threshold). Agreement with experiment is satisfactory at small and middle energies, however, at large energies the calculated cross section is smaller than the experimental one by about 10%. The calculations in the CADW approximation (Loch *et al* 2002) are also presented in figure 3. We see good agreement for the direct ionization data, but the maximum CADW total cross section is slightly smaller than the present one. That means that the excitation cross sections of the autoionization levels are rather different in the maximum range.

3.3. Kr XV

The comparison with the experimental data (Khouilid *et al* 2001a) is presented in figure 5. The first threshold is clearly observed around 478 eV, which is 16 eV below the theoretical

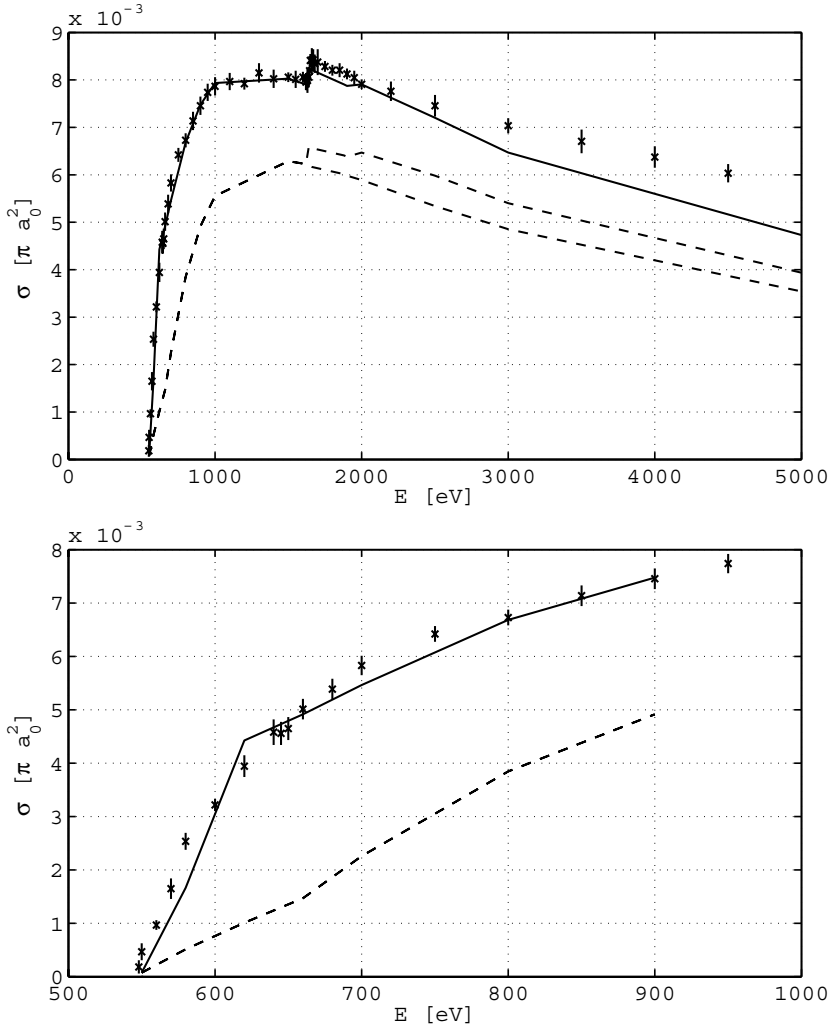

Figure 6. The same as figure 4 for Kr XVI from the $3s^2 3p^6 3d^3$ state.

ground-state threshold (table 3). This energy difference indicates that the metastable state is present in the primary ion beam. The contribution of the 3s and 3p excitation followed by autoionization is about 50% of the total cross section near the threshold. Around 1645 eV, a weak contribution is observed due to the excitation autoionization process involving the 2p–3d transition. At the middle and large energies the contribution of the autoionization levels from the 2s, 2p shells is comparable with that from the 3s, 3p shells. The agreement with the experimental data is satisfactory at $E < 1$ keV, however, the calculated cross section is larger than the experimental one at large energies (about 10%).

3.4. Kr XVI

The comparison with the experimental data (Khouilid *et al* 2001a) is presented in figure 6. The measurement shows good agreement between the observed threshold (542 eV) and

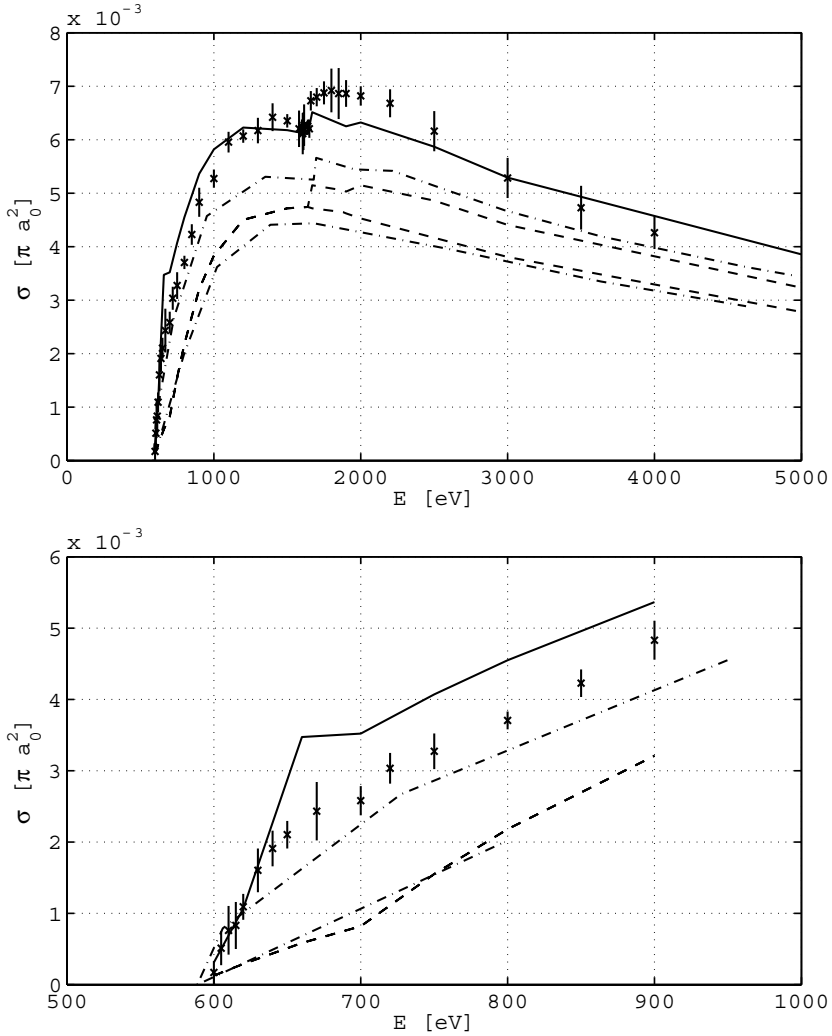

Figure 7. The same as figure 3 for Kr XVII from the $3s^2 3p^6 3d^2$ state.

the calculated ionization energy of the 3d ground state. At middle and large energies the contribution of the autoionizing levels with holes in the 2s, 2p shells is about one half of those from the 3s, 3p shells. The agreement with the experimental data is satisfactory at $E < 2$ keV, however, the calculated cross section is smaller than the experimental one at large energies (about 10%).

3.5. Kr XVII, Kr XVIII

The comparison with the experimental data (Khouilid *et al* 2001a) is presented in figures 7, 8. The first threshold of Kr XVII is observed around 585 eV, which is 8 eV below the ground-state theoretical threshold. This is the signature of the ^{3}P, ^{1}D, ^{1}G, metastable states which is located 6–9 eV above the ground-state level. Around 1655 eV the threshold excitation autoionization of the 2p state is clearly observed. This contribution increases the total cross section by

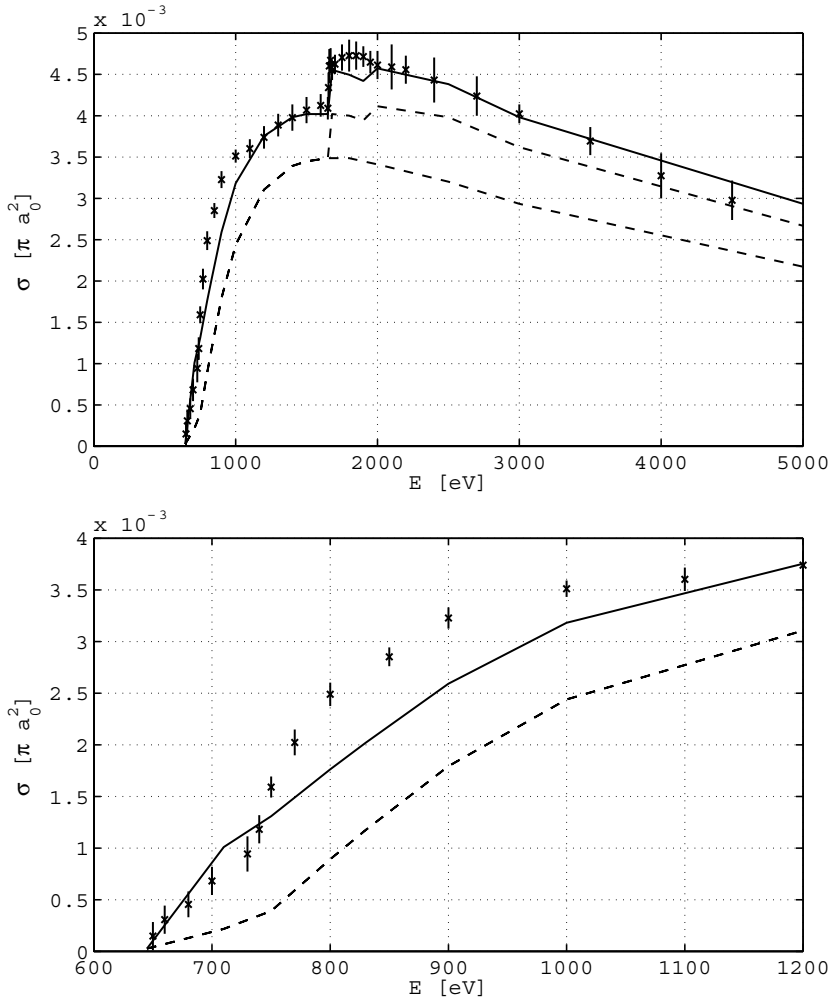

Figure 8. The same as figure 4 for Kr XVIII from the $3s^2 3p^6 3d$ state.

some 10%. The measured cross section of Kr XVIII is well below the threshold observed at 637 eV. This value is in good agreement with the calculated 3d ground state. At around 750 eV contributions of direct ionization and of excitation from the 3p shell clearly compete. For both ions excitation from the 3s, 3p shells is the dominating process at $E < 750$ eV (similar to the previous ions). At middle and large energies the contribution of the autoionizing levels from the 2s, 2p shells is about equal to the excitation contribution from the 3s, 3p shells or greater (for Kr XVIII). The agreement with the experimental data is satisfactory.

The calculations in the CADW approximation (Loch *et al* 2002) are also presented in figure 7. As in the case of Kr XIII, there is good agreement for the direct ionization data. However, the total CADW cross section is smaller than the present one in the whole energy range. The reason behind this difference requires more detailed investigations. It is possibly connected with the contribution of the highly excited autoionizing $3snl$, $3pnl$ levels (in this work the asymptotic $1/n^3$ law was used to obtain the summed contribution of these levels).

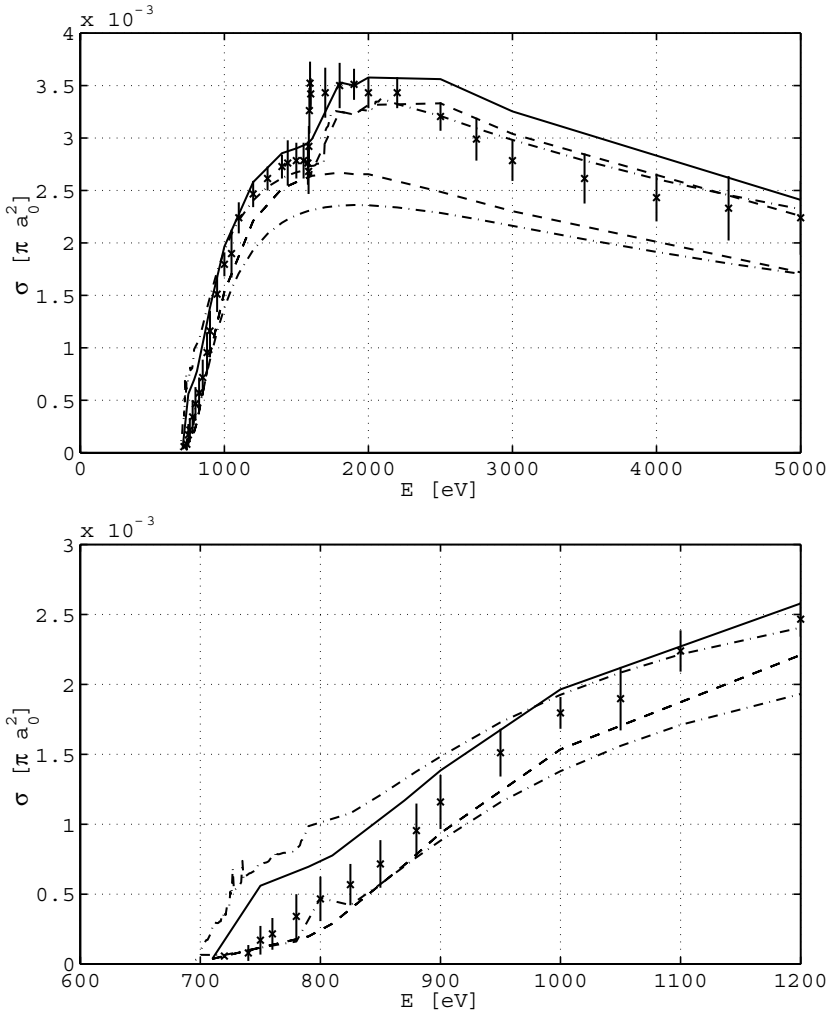

Figure 9. The same as figure 1 for Kr XIX from the metastable $3s^2 3p^5 3d$ state.

3.6. Kr XIX

The comparison with the experimental data (Khouilid *et al* 2001a) and the calculations from (Teng *et al* 2000) is presented in figure 9. Kr XIX belongs to the argon isoelectronic sequence. The first threshold is observed around 703 eV, which is about 80 eV below the ground-state ionization threshold of 784.4 eV (see table 2(b)). It is clear that the primary ion beam contains a dominant population of the metastable configuration $1s^2 2s^2 2p^6 3s^2 3p^5 3d$. In our calculations it was assumed that all ions are in this state.

The contribution of the autoionization from 3s, 3p shells is much smaller than the contribution of the excitation from 2s, 2p shells (at $E > 1.5$ keV) because of the narrow energy band connected with the autoionizing levels ($n > 9$ for 3p, see table 4). In the threshold region 700–850 eV, however, the excitation from 3p results in too large an ionization cross section, which may be connected with the role of exchange. Again there are some differences (about 10%) between the present calculations and the results (Teng *et al* 2000).

4. Summary

In the present paper, we report on the calculation of a single ionization cross section for Kr XI–XIX ions. Direct ionization, which is generally the dominating process, and excitation–autoionization processes are taken into account in the average-configuration Coulomb–Born approximation. Direct ionization decreases regularly with increasing charge state, according to the reducing number of active outer-shell electrons. On one hand, with excitation autoionization processes the contribution of $3s[3d^m]$, $3p[3d^m] \rightarrow [3d^m]nl$ transitions, which dominates the ionization signal close to the ionization threshold, is seen to decrease with m increasing, due to increases in the principal quantum number n for which autoionization is possible. On the other hand, the relative importance of $2s, 2p \rightarrow 3d$ transitions (configuration $[Ar]3d^m$, $m = 0$–8) increases since the number of 3d vacancies increases.

The calculated cross sections are overall in good agreement with the experimental data, the discrepancy being of the order of 10%. The possible error can be connected with the error of the 'averaged' description of the autoionization states.

Acknowledgment

This work was supported in part (I Beigman and L Vainshtein) by RFBR (projects 00-02-17825, 03-02-16053).

References

Barué C, Biri S, Cherkani-Hassani S, Gealens M, Loiselet M and Ryckewaert G 1998 *Rev. Sci. Instrum.* **69** 764

Blanke J H, Fricke B and Finkbener M 1992 Database *Plasmarelevante Atomare Daten* (Germany: University of Kassel)

Duponchelle M, Zhang M, Oualim E M, Bélenger C and Defrance P 1995 *Nucl. Instrum. Methods Phys. Res.* A **364** 159

Grant I P, McKenzie B J, Norrington P H, Mayers D F and Pyper N C 1980 *Comput. Phys. Commun.* **21** 207

Janev R K 1993 Summary Report of the IAEA Technical Committee Meeting on Atomic and Molecular Fusion Reactor Technology *Report INDC* (NDS-277) (Vienna: IAEA)

Kelleher D E, Wiese W L, Martin W C, Olsen K, Musgrove A, Mohr P J, Sugar J, Reader J, Sansonetti C J and Dalton G R 2002 National Institute of Standards and Technology (version 2) http://physics.nist.gov/cgi-bin/AtData/main_asd

Khouilid M, Cherkani-Hassani S, Rachafi S, Teng H and Defrance P 2001a *J. Phys. B: At. Mol. Opt. Phys.* **34** 1727

Khouilid M, Cherkani-Hassani S, Adimi N, Rachafi S and Defrance P 2001b *J. Phys. B: At. Mol. Opt. Phys.* **34** 3239

Loch S D, Pindzola M S, Balance C P, Griffin D C, Mitnik D M, Badnell N R, O'Mullane M G, Summers H P and Whiteford A D 2002 *Phys. Rev.* A **66** 052708

Oualim E M, Duponchelle M and Defrance P 1995 *Nucl. Instrum. Methods Phys. Res.* B **98** 150

Shevelko V P and Vainshtein L A 1993 *Atomic Physics for Hot Plasmas* (London: Institute of Physics Publishing)

Sobelman I I, Vainshtein L A and Yukov E A 1995 *Excitation of Atoms and Broadening of Spectral Lines (Springer Series on Atoms and Plasmas vol 15)* (Berlin: Springer)

Sugar J and Musgrove A 1991 *J. Phys. Chem. Ref. Data* **20** 859

Teng H, Defrance P, Chen C and Wang Y 2000 *J. Phys. B: At. Mol. Opt. Phys.* **33** 463

Younger S M 1982 *Phys. Rev.* A **26** 3177